Assignment of capacitance spectroscopy signals of CIGS solar cells to effects of non-ohmic contacts

Johan Lauwaert,[1,*] Lisanne Van Puyvelde,[1] Jeroen Lauwaert,[2] Joris W. Thybaut,[2] Samira Khelifi,[3] Marc Burgelman,[3] Fabian Pianezzi,[4] Ayodhya N. Tiwari,[4] and Henk Vrielinck[1]

[1]*Department of Solid State Sciences, Ghent University, Krijgslaan 281-S1, 9000 Gent, Belgium*

[2]*Laboratory for Chemical Technology (LCT), Ghent University, Krijgslaan 281-S5, 9000 Gent, Belgium*

[3]*Department of Electronics and Information Systems (ELIS), Ghent University, St.-Pietersnieuwstraat 41, B-9000 Gent, Belgium*

[4]*Laboratory for Thin Films and Photovoltaics, Swiss Federal Laboratories for Materials Science and Technology (Empa), Ueberlandstrasse 129, CH-8600 Duebendorf, Switzerland*

(Dated: February 25, 2013)

Abstract

We report evidence for the idendification of the capacitance transients detected at room temperature for thin-film photovoltaic cells with CIGS absorbers as an additional non-ohmic contact in the structure with a time constant larger than that of the solar cell pn-jucntion. The N1 signal was recently interpreted as a back contact barrier for which the RC-like time constant is smaller than the time constant of the junction. In this work we unite these experimental observations in one model. Since for a Mo/CIGS/CdS/ZnO solar cell several interfaces are connected in series, we introduce the idea of modeling capacitance spectroscopy signals based on RC-circuits in series for each interface. It is shown that the distinct features observed in capacitance spectroscopy of CIGS solar cells can be mimicked using this circuit as an electrical model. The differential equation for this structure as a function of time is solved numerically. It is inherent to the model that the transients in such a structure are voltage transients over each of the interfaces and that the transients are coupled. These findings question the practical use of capacitance spectroscopy for direct measurement of defects in the absorber layer.

PACS numbers: 71.55.Cn

*Electronic address: Johan.Lauwaert@UGent.be

I. INTRODUCTION

In general, the lower efficiency of thin-film photovoltaic cells in comparison with (multi-) crystalline Si cells should be compensated by their lower production/material cost. Recently, laboratory efficiencies of over 20% have been reached with $CuIn_{1-x}Ga_xSe_2$ (CIGS) solar cells [1], approaching those of Si technology, and very efficient cells on flexible substrates have also been demonstrated [2]. This makes CIGS the most promising thin-film type cells, albeit that very large scale application may be prevented by the limited resources in (and competitive markets for) In. It is generally believed that intrinsic defects and impurities in the CIGS absorber layer have an impact on carrier recombination − hence also on the cell efficiency − and that further optimization requires knowledge and control over these defects [3]. Next to photoluminescence, capacitance based (quasi) spectroscopic techniques, like deep-level transient spectroscopy (DLTS) and admittance spectroscopy (AS) are widely used to study defects in the absorber layer [4–17] making use of the fact that free carrier trapping and emission in deep defect levels [20, 21] contribute to the depletion capacitance (transients) of the solar cell p-n junction.

Figure 1 shows as an example DLTS (Fig. 1a) and AS (Fig. 1c) spectra of a $n^+ - ZnO/n - CdS/p - CIGS/Mo$ solar cell structure. They typically exhibit two signals. At low temperature (DLTS and AS) a signal labeled N1 is usually observed, whose appearance seems independent on the manufacturing technology (but whose properties may vary strongly when changing cell layer thicknesses and/or synthesis conditions)[3]. In conventional DLTS this signal often is negative, as is the case in Fig. 1a, where we adopt the convention to label the capacitance transients corresponding to majority carrier emission from traps as positive ($C_r = C(\infty) > C(t)$ short after the pulse switch off, for $V_r < V_p$). Besides an assignment to electrically active defect levels also alternative explanations have been given for N1 like temperature dependent carrier hopping [18] or Maxwell-Wagner polarization of the absorber [19] based on AS. A second signal appears at higher temperatures (lower frequencies) in AS (see Fig. 1c) and gives rise to slow capacitance transients near room temperature (RT) in DLTS (see Fig. 1a and b). Following Scheer and Schock [3] we label this signal here N2.

Carrier trapping and emission by deep levels is, however, not the only source of signals in DLTS and AS. Recently, in order to explain the anomalies of the N1 signal in AS, Eisen-

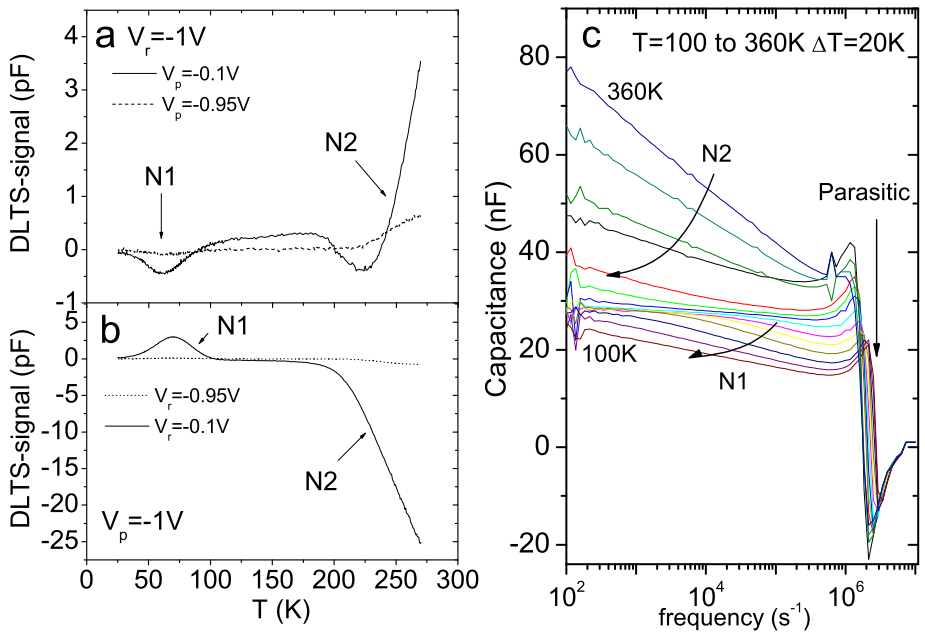

FIG. 1: (a) Conventional DLTS spectra (b) Complementary DLTS spectra (c) Capacitance as a function of frequency (AS). The N1 signal is seen at $\approx 50K$ in DLTS and the N2 signal at $T > 230K$. The features seen at $\nu > 500kHz$ in AS are due to parasitic effects.

barth et al. [9] proposed to assign this signal to the non-ideal back contact (reverse polarized Schottky diode). Subsequently, comparing the signals after normal ($V_r < V_p$) and reversed ($V_p < V_r$) pulses we identified the characteristics of a non-ideal contact in DLTS [22] and demonstrated for two cells with different buffer layers that the properties of the N1 signal are i) incompatible with an assignation to defects, and ii) in very good agreement with those expected for a non-ideal (back) contact [23]. Meanwhile we verified that in all cells we measured so far the N1 DLTS signal indeed exhibits properties typical for a non-ideal contact. In the present paper, the properties of the N2 signal are examined and are also found to be compatible with an attribution to a non-ohmic contact. The equivalent circuit model developed by Lauwaert et al. [22, 23] is extended with a second contact. This model is found able to explain the shape of the spectra in a qualitative way. The implications of assigning both N1 and N2 signals to contact rather than to defect properties are discussed.

II. EXPERIMENTAL DETAILS AND METHODOLOGY

Since in electrical properties of CIGS solar cells slow varying processes are observed [3], it is often not evident to interpret DLTS spectra as a fingerprint for a solar cell in a certain metastable configuration. One might expect that these slow varying processes continue and influence the observations at a faster time scale. To prevent unkown time constants from influencing our measurements, we suggest to record capacitance transients in a reproducible way.

For the N2 signal at room temperature a much larger time-constant is observed than the filtering time constants one typically uses for the observation in DLTS spectroscopy. However one would prefer to perform measurements of transients that are reproducible, which is possible if the cell is in a steady state regime. Therefore we try to estimate the waiting time and the number of cycles needed to record transients independent of the history of the cell. Let us consider a general observable parameter P that converges to zero with a time constant τ and adapts directly to an external change ΔP. For simplicity we take the same time constant for the response to a positive or negative change. One applies a sequence of pulses $+\Delta P, -\Delta P$, with a period $2T$ to this system. The first cycle starting from $\Delta P + P_0$ for $t = 0$, can be written as $P_1(t) = (\Delta P + P_0)e^{-\frac{t}{\tau}}$. Herein the parameter P_0 is determined by the history of the system. Since T is not necessarily much larger than τ so that the second period cannot be interpreted as starting from the equilibrium situation, the second cycle should be written as: $P_2(t) = P_0 e^{-\frac{T}{\tau}} e^{-\frac{t}{\tau}} + \Delta P \left(e^{-\frac{T}{\tau}} - 1\right) e^{-\frac{t}{\tau}}$, which for simplicity was assumed to adopt a new time origin at $t = T$. In a similar way the general cycle i can be written as:

$$P_i(t) = \left[P_0 e^{-\frac{(i-1)T}{\tau}} + (-1)^{i-1} \sum_{j=0}^{i-1} \left(-e^{-\frac{jT}{\tau}}\right) \Delta P\right] e^{-\frac{t}{\tau}} \tag{1}$$

Where t starts at the beginning of the i^{th} cycle. In such a situation reproducible measurements can only be observed if $e^{-\frac{iT}{\tau}} \ll 1$. For a time-constant in the order of 1 hour ($\tau = 3600s$), which is often suggested as waiting time to bring a solar cell in relaxed or light-soaked configuration, iT should be larger than 2.5×10^4s $\approx 7\tau$ for a deviation of 0.1%. In this work we perform isothermal DLTS measurements recording the transient after 10 periods of $T = 5000$s. This method makes it possible to measure the capacitance transient in a steady state regime. Such a sequence of pulses allows us to measure and characterize

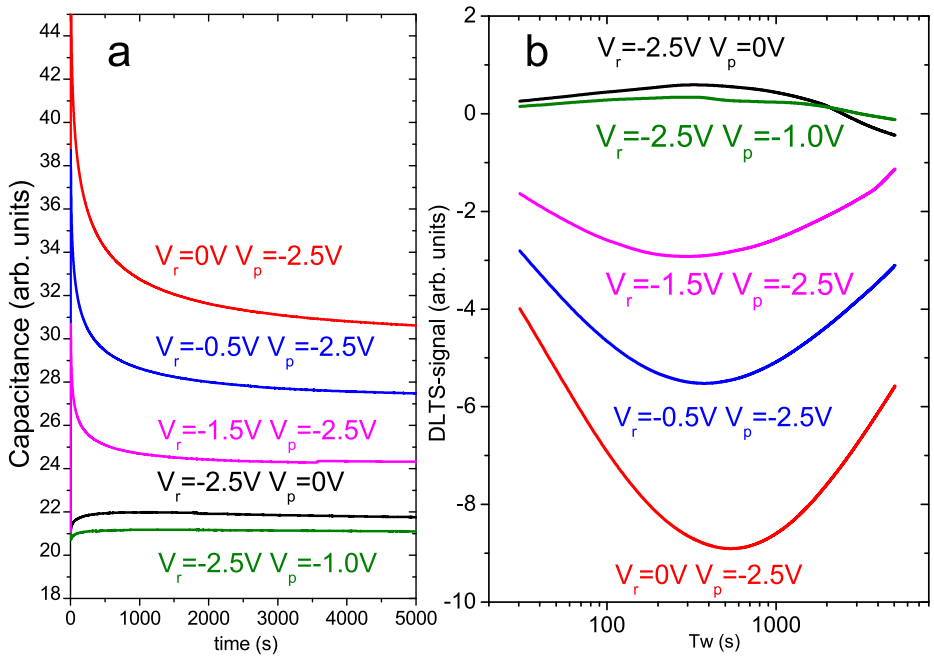

FIG. 2: (a) Transient observed at room temperature on a CIGS solar cell (b) Fourier transform analysis of the recorded transients.

the typical properties of the N2-signal.

Capacitance transients were recorded with an SR-830 Lock-In amplifier [6] and Fourier transformed to obtain isothermal DLTS spectra.

III. RESULTS AND DISCUSSION

Figure 2a shows the capacitance transients observed at room temperature for a CIGS state of the art solar cell [26] for different pulse V_p and reverse bias V_r values. For each of these transients the cell was stabilized for $50ks$ in the dark while applying a series of pulses. The isothermal DLTS spectra (Fig. 2b) are calculated from the individual transients via Fourier analysis [28]. Since the N2 signal can be observed in DLTS and AS at room temperature this increasing capacitance after a negative voltage step $V_r < V_p$ ($\Delta V < 0$) is the conventional isothermal DLTS spectrum of the N2 signal. The complement signal with $V_r > V_p$ ($\Delta V > 0$) has a much larger amplitude and the time constants for conventional and

complementary signals converge to one another for small pulse heights. These observations are in agreement with our recent analysis [22] of a signal originating from an RC-like contact with a time constant τ_2 larger than that of the junction τ_0. In order to distinguish this from emission and capture by deep-level defects, measurements need to be made in a steady state regime. Only for such a regime the properties of the two models have been calculated. As we evaluated the properties of the alternative origins of DLTS signals (i) carrier trapping and emission by deep defects and (ii) RC-like contacts only in steady state regime, it is important to ensure that the measurements indeed follow this regime.

Recently we demonstrated that the N1 signal in DLTS also shows very good agreement with the model proposed for an additional interface in the layered structure [22, 23]. Testing of this model was extended for more cells. We found that all negative N1 DLTS signals can be described with an RC-like contact, confirming that the discussion is not a unique finding for a limited number of specimens. Contrary to the N2 signal the N1 signal has a time constant τ_1 that is smaller than that of the junction τ_0.

If one wants to observe both effects in one device it is necessary to introduce two additional interfaces besides the junction with the lowest capacitance that determines the total capacitance at high frequency ($\nu = 1$Mhz), as will be clarified below. We propose to model the total structure as an equivalent circuit shown in figure 3a. The interfaces are labeled A,B,C and the time constants 0,1 and 2. We deliberately use different labels to emphasize that although each interface is responsible for one time constant, it is not possible to find out which interface is responsible for what time constant when restricting to electrical measurements. Since the time constants for both the N1 and N2 features show thermal activation we introduce a Boltzmann activation for each of the interfaces i, whose time constant can be written as:

$$\tau_i = R_i C_i = \tau_{i0} \exp\left(\frac{-E_i}{k_B T}\right) \tag{2}$$

as shown in figure 3b. We assume that each of the interfaces can be interpreted as an electrically equivalent circuit of a resistor $R_i = R_{i,0} \exp\left(-\frac{E_i}{k_B T}\right)$ and a temperature independent capacitor C_i in parallel and bulk materials that are modeled as a resistor r_k (see figure 3 a). The bulk resistors r_k are also kept constant as a function of temperature. The bulk materials k, whose resistance is mainly determined by the one with lowest free carrier concentration, i.e. the CIGS absorber as one expects for normal CV behaviour $\left(\frac{dC}{dV} > 0\right)$, may be regarded as a single resistor $r = \sum_k r_k$.

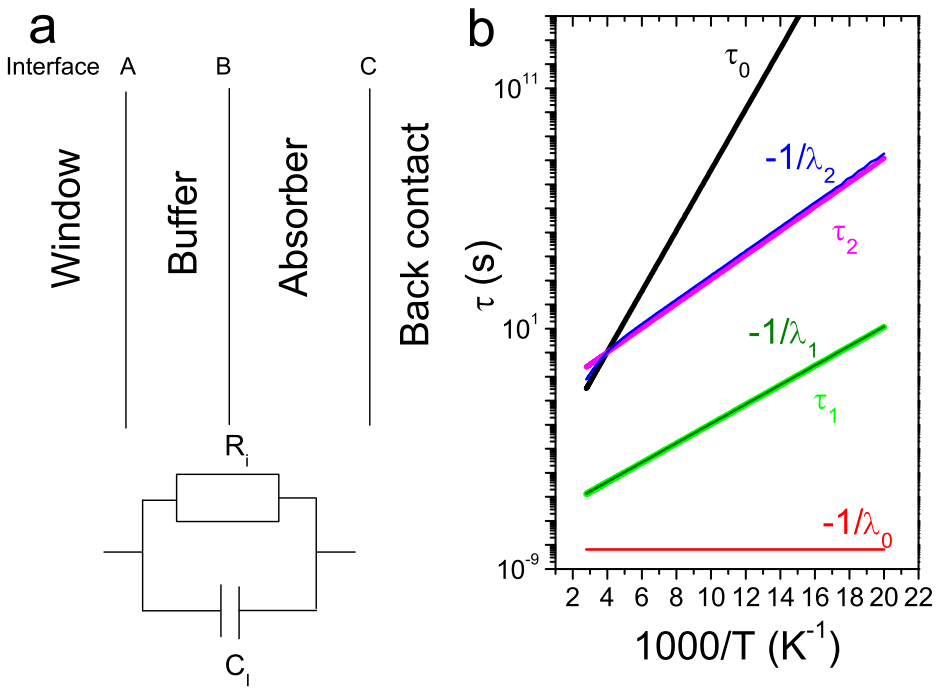

FIG. 3: (a) Graphical representation of a thin film solar cell consisting of a series of layers (i.e. window, buffer, absorber, back contact). Each of the interfaces i between the layers ,for $i = A, B, C$, is modeled as a parallel connection of a resistor R_i and capacitor C_i. (b) Time constants of each of the interfaces i, $\tau_i = R_i C_i$ as a function of temperature, calculated using a Boltzmann-activation, and the corresponding time constants in the potential drops calculated for the total structure over each of the interfaces $-\frac{1}{\lambda_l}$.

To model the transient behavior in DLTS we solve the coupled differential equations for the potential drop over each of the three interfaces for each temperature, assuming that the capacitance measured over the total structure is mainly determined by the potential drop over the junction V_0 for sufficiently high frequency [23], since $C_0 \ll C_{i\neq 0}$. The DLTS-signal is taken as proportional to V_0 as demonstrated in Ref. 22, while the capacitance as a function of frequency (AS) is calculated via the capacitance of the total structure. The potential drop over one of the interfaces i can be written as:

$$\frac{dV_i}{dt} = \frac{V^{TOT}}{rC_i} - \frac{\sum_j V_j}{rC_i} - \frac{V_i}{R_i C_i} \tag{3}$$

Which results in a set of first order differential equations

$$\frac{dV_i}{dt} = \sum_j A_{ij} V_j + b_i$$

with the elements in the matrix

$$A_{ij} = -\frac{1}{rC_i} - \frac{\delta_{ij}}{\tau_i}$$

Herein this structure is kept at a constant bias $V^{TOT} = \sum_i V_i + \sum_k V_k$, which is V_r during observation and V_p during the pulse.

The set of first order differential equations (3) results in a solution for V_i of the form:

$$V_i = \sum_l C_{il} e^{\lambda_l t} + b_i \tag{4}$$

with λ_l, $l = 0, 1, 2$, the eigenvalues of the matrix A. Thus we see that the potential drop changes exponentially with time over each of the interfaces, that each of the time constants is in principle observable over any of the interfaces, and, since $\lambda_l < 0$, the potential drops converge to an equilibrium situation

$$V_i\,(t = +\infty) = \frac{R_i V^{TOT}}{\sum_j R_j + r} \tag{5}$$

This set of first order differential equations can be solved numerically, which has been done in all simulations below. The eigenvalues are solutions of $det(\overleftrightarrow{A} - \lambda_i . \overleftrightarrow{1}) = 0$ and are explicitly calculated in appendix A. In the situation where $r \ll R_i \quad \forall i$, the largest eigenvalue can be approximated by:

$$\lambda_0 \approx -\frac{1}{r} \sum_i \frac{1}{C_i} \tag{6}$$

For $\tau_1 \ll \tau_i \quad i \neq 1$ the other two eigenvalues of this system can be written as:

$$\lambda_1 \approx -\frac{1}{\tau_1} \tag{7}$$

$$\lambda_2 \approx -\left(\frac{R_0 + R_2}{C_0 + C_2}\right) \frac{1}{R_0 R_2} \tag{8}$$

For the slowest time constant, $-\frac{1}{\lambda_2}$ (Eq. 8), two regimes as function of temperature ($\tau_0 < \tau_2$ and $\tau_2 < \tau_0$) can be distinguished as discussed by Lauwaert et al. [22]. The fastest λ_0 (Eq. 6) is in our assumption inversely proportional to the series resistance and temperature independent. The fact that r is chosen much smaller than $R_i \quad , \forall i$, makes its effect on the

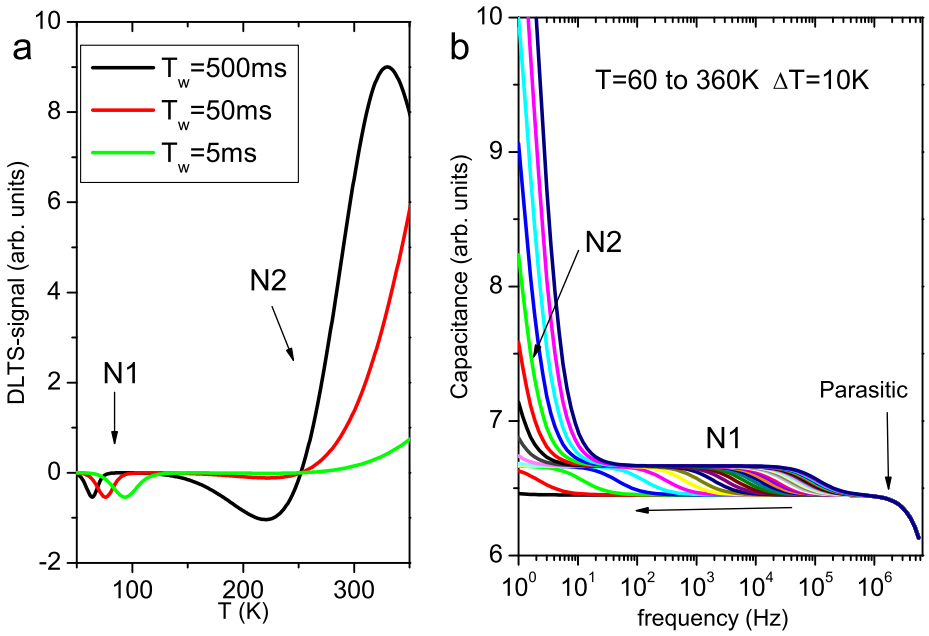

FIG. 4: (a) DLTS spectra and (b) Capacitance as function of frequency (AS) as calculated based on the time constants shown in figure 3b and a temperature independent capacitance for each of the interfaces C_i.

DLTS spectrum negligible. However, in admittance spectroscopy it might be observable at the highest frequencies as a parasitic effect, as discussed in Ref. [27]. The transient mainly determined by the interface with time constant τ_1 : $\exp(-\lambda_1 t)$ (Eq. 7) is temperature dependent and will result in a negative DLTS signal, with RC like properties as described in Ref. [23]. The combination of these assumptions makes it possible to simulate capacitance spectra (both DLTS and AS) with certain settings based on only ten different parameters τ_{i0}, E_i, C_i $(i = 0, 1, 2)$ and r.

Figure 4a shows a DLTS spectrum calculated using the Boltzmann activation in the time constants that, as mentioned above, for simplicity has been assigned to an activation in the resistor and a constant capacitance as shown in figure 3b. We observe that such a series structure of interfaces results in a sequence of peaks at the temperature where the time constant $-\frac{1}{\lambda_l}$ corresponds to the observation time. In contrast with normal emission peaks

from deep levels in the band gap of one of the layers, where the amplitude is dependent on the concentration and spatial distribution, the amplitudes simply depend on the parameters in the model.

Calculations are made using the Fourier-Transform technique for the observation of the DLTS-spectrum [28]. At low temperature we observe an N1-like signal with a time constant τ_2 in relation with the back contact. At higher temperature we calculate a broader peak in agreement with the N2 signal.

In AS, calculated as the quiescent capacitance of the total structure in equilibrium, the same sequence of steps can be observed, coinciding with the eigenvalues of the circuit as expected. At high frequencies we observe the series resistance as a parasitic effect in the spectrum [27]. This parasitic step corresponds with a frequency $\nu = \frac{\lambda_0}{2\pi}$. At lower frequencies we can observe the temperature dependence of the resonance frequencies corresponding with λ_1 and λ_2, in a typical capacitance frequency plot corresponding with N1 and N2. Note that at $1MHz$ the capacitance corresponds with C_0, confirming our assumption that in DLTS the capacitance is mainly determined by the junction with the smallest capacitance.

One could note that by introducing a thermal activation in the time constants only one additional contact also could result in two DLTS signals: one observed in the temperature range for which the time constant of the additional contact τ_1 is larger than the time constant of the junction τ_0 and a signal with the opposite sign for the temperature region for which τ_1 is smaller than τ_0. Since experimentally the activation energy of N1 is typically lower than the activation of N2 [3], we expect the N2 signal at higher temperature than N1, in excellent agreement with literature [3]. However, since we introduced only one additional contact in the structure, this model requires that this N2 signal is always faster than the N1 signal, which is contrary to our observations and the typical admittance spectra observed on such structures [3]. Thus, for generating a series of time constants mimicking the typical properties of a CIGS solar cell, one needs an RC contact that deviates from a simple Boltzmann activation or to introduce an additional contact. Since a Mo/CIGS/CdS/ZnO structure has three interfaces (Fig. 3 a) we propose to follow the option of an additional non-ohmic contact in the model.

IV. CONCLUSIONS

Based on the equivalent circuit of a series chain of interfaces and bulk materials, we can calculate spectra exhibiting the typical properties observed for thin film solar cells. The two major features labeled N1 and N2 were modeled and thus the typical form of the complete spectrum can be explained via these calculations. The correlation between the two is explained as a series chain of interfaces each with an RC-like time constant. Experimentally it is shown that both the N1 and N2 signals obey the typical properties for an RC-like contact. The remarkable good agreement of this model with typical capacitance spectra suggest that those techniques are not straightforward methods to identify defects in advanced layered structures. Even though DLTS and AS spectroscopy were originally invented to measure charging and decharging of defects and thermodynamically one expects the presence of defects, the main features observed are most probably related with non-ohmic contacts in the structure.

Acknowledgments

The authors acknowledge the special university fund of UGent (BOF-01N01611) for financial support. S. Khelifi acknowledges the financial support of the IWT-SBO project SiLaSol sponsored by The Institute for the Promotion of Science and Technology.

APPENDIX A: CALCULATION OF TIME-CONSTANTS

The negative eigenvalues $-\lambda_i$ of the matrix A with matrix-elements $A_{ik} = -\frac{1}{rC_i} - \frac{\delta_{ik}}{R_iC_i}$ are solutions of the equation:

$$\prod_i \left[\frac{1}{rC_i} + \frac{1}{R_iC_i} - \lambda\right] + 2\prod_i \frac{1}{rC_i} - \sum_{i\neq j\neq k\neq i} \left(\frac{1}{rC_Ai} + \frac{1}{R_iC_i} - \lambda\right) \frac{1}{rC_j}\frac{1}{rC_k} = 0 \qquad \text{(A1)}$$

In our case that $i = 0, 1, 2$ (3-interfaces), this leads to:

$$\lambda^3 - \left(\sum_i \left(\frac{1}{rC_i} + \frac{1}{\tau_i}\right)\right)\lambda^2 + \sum_{i\neq j}\left(\frac{1}{rC_i} + \frac{1}{\tau_i}\right)\frac{1}{\tau_j}\lambda - \frac{1}{\tau_0\tau_1\tau_2} - \sum_{i\neq j\neq k\neq i} \frac{1}{rC_i\tau_j\tau_k} = 0 \qquad \text{(A2)}$$

for $r \ll R_i$ this equation further reduces to:

$$\lambda^3 - \sum_i \frac{1}{rC_i}\lambda^2 + \sum_{i\neq j} \frac{1}{rC_i\tau_j}\lambda - \sum_{i\neq j\neq k\neq i} \frac{1}{rC_i\tau_j\tau_k} = 0 \qquad \text{(A3)}$$

with the largest eigenvalue

$$-\lambda_0 = \frac{1}{r}\sum_i \frac{1}{C_i} \tag{A4}$$

The other two eigenvalues are solutions of the quadratic equation:

$$\sum_i \frac{1}{C_i}\lambda^2 - \sum_{i\neq j} \frac{1}{C_i\tau_j}\lambda + \sum_{i\neq j\neq k\neq i} \frac{1}{C_i\tau_j\tau_k} = 0 \tag{A5}$$

If $\tau_1 \ll \tau_2, \tau_0$ a second solution is

$$-\lambda_1 = \frac{1}{\tau_1} \tag{A6}$$

And the last solution can thus be written as:

$$-\lambda_2 = \frac{\sum_{i\neq j\neq k\neq i} \frac{\tau_1}{C_i\tau_j\tau_k}}{\sum_i \frac{1}{C_i}} \approx \frac{\frac{1}{C_0\tau_2} + \frac{1}{C_2\tau_0}}{\sum_i \frac{1}{C_i}} \tag{A7}$$

which for $C_1 \gg C_2, C_0$ can be reduced to:

$$-\lambda_2 = \frac{\frac{1}{R_2} + \frac{1}{R_0}}{C_0 + C_2} \tag{A8}$$

that were used in Eqs. 6,7 and 8. Thus in the situation where one of the contacts (here $i = 1$) can be seen as a small perturbation on the other two ($i = 0, 2$): $C_1 \gg C_2, C_0$ and $\tau_1 \ll \tau_2, \tau_0$ and where the series resistance r is small compared to the other resistances R_i, three well-seperated eigenvalues are expected.

---

[1] P. Jackson, D. Hariskos, E. Lotter, S. Paetel, R. Wuerz, R. Menner, W. Wischmann, and M. Powalla, New world record efficiency for Cu(In, Ga)Se_2 thin-film solar cells beyond 20%, Progress in Photovoltaics: Research and Applications,**19(7)** (2011) 894897.

[2] A. Chirilă, S. Buecheler, F. Pianezzi, P. Bloesch, C. Gretener, A. R. Uhl, C. Fella, L. Kranz, J. Perrenoud, S. Seyrling, R. Verma, S. Nishiwaki, Y. E. Romanyuk, G. Bilger and A. N. Tiwari, Highly efficient Cu(In, Ga)Se_2 solar cells grown on flexible polymer films, Nature Materials 10 (2011) 857861 .

[3] R. Scheer and H.W. Schock , Chalcogenide Photovoltaics, Physics, Technology, and Thin Film Devices, Wiley (2011).

[4] M. Cwil, M. Igalson, P. Zabierowski, S. Siebentritt, Charge and doping distributions by capacitance profiling in Cu(In, Ga)Se_2 solar cells, J. Appl. Phys. **103(6)** (2008) 063701.

[5] F. Engelhardt, M. Schmidt, T. Meyer, O. Seifert, U. Parisi and U. Rau, Metastable electrical transport in Cu(In, Ga)Se_2 thin films and ZnO/CdS/Cu(In,Ga) Se_2 heterostructures Physics Letters A **245(5)** (1998) 489-493.

[6] J.T. Heath, J.D. Cohen and WN. Shafarman, Bulk and metastable defects in $CuIn_{1-x}Ga_xSe_2$ thin films using drive-level capacitance profiling, J. Appl. Phys. **95(3)** (2004) 1000.

[7] M. Igalson, P. Zabierowski, A. Romeo and L. Stolt, Reverse-bias DLTS for investigation of the interface region in thin film solar cells, Opto-Electronics Review **8(4)** (2000) 346-349.

[8] M. Igalson, A. Urbaniak and M. Edoff, Reinterpretation of defect levels derived from capacitance spectroscopy of CIGSe solar cells, Thin Solid Films **517(7)** (2009) 2153.

[9] T. Eisenbarth, T. Unold, R. Caballero, C.A. Kaufmann and H.W. Schock, Interpretation of admittance, capacitance-voltage, and current-voltage signatures in Cu(In, Ga)Se_2 thin film solar cells, J. Appl. Phys. **107** (2010) 034509.

[10] M. Igalson, P. Zabierowski, D. Przado, A. Urbaniak, M. Edoff and W.N. Shafarman, Understanding defect-related issues limiting efficiency of CIGS solar cells, Solar Energy Mater. Sol. Cell. **93** (2009) 1290.

[11] M. Igalson and P. Zabierowski, Transient capacitance spectroscopy of defect levels in CIGS devices, Thin Solid Films **361-362** (2000) 371.

[12] M. Igalson, M. Wimbor and J. Wennerberg, The change of the electronic properties of CIGS devices induced by the 'damp heat' treatment, Thin Solid Films **403-404** (2002) 320.

[13] P. Zabierowski, K. Stankiewicz, A. Donmez, F. Couzinie-Devy and N. Barreau, Systematic study of the complex structure of N-1 Deep Level Transient Spectroscopy signal in Cu(In, Ga)Se_2 based heterojunctions, Thin Solid Films **519** (2011) 7485.

[14] L.L. Kerr, S. Sheng, B. Li, S.W. Johnston, T.J. Anderson, O.D. Crisalle, W.K. Kim, J. Abushama and R.N. Noufi, Investigation of defect properties in Cu(In, Ga)Se_2 solar cells by deep-level transient spectroscopy, Solid-State Electronics **48** (2004) 1579.

[15] P. Zabierowski and M. Edoff, Laplace-DLTS analysis of the minority carrier traps in the Cu(In, Ga)Se_2-based solar cells, Thin Solid Films **480-481** (2005) 301.

[16] Z. Djebbour, A. Darga , A. Migan Dubois, D. Mencaraglia, N. Naghavi, J.-F. Guillemoles and D. Lincot, Admittance spectroscopy of cadmium free CIGS solar cells heterointerfaces, Thin Solid Films **511-512** (2006) 320.

[17] S. Khelifi, A. Belghachi, J. Lauwaert, K. Decock, J. Wienke, R. Caballero, C.A. Kaufmann

and M. Burgelman, Characterization of flexible thin film CIGSe solar cells grown on different metallic foil substrates, Energy Procedia **2(1)** (2011) 109-117.

[18] U. Reislöhner, H. Metzner and C. Ronning, Hopping Conduction Observed in Thermal Admittance Spectroscopy, Phys. Rev. Lett. **104** (2010) 226403.

[19] U. Reislöhner and C. Ronning, Maxwell-Wagner polarization in $Cu(In, Ga)(S, Se)_2$, Appl. Phys. Lett. **100** (2012) 252111.

[20] S. Lany and A. Zunger, Intrinsic DX centers in ternary chalcopyrite semiconductors, Phys. Rev. Lett. **100(1)** (2008) 016401.

[21] S. Lany and A. Zunger, Light- and bias-induced metastabilities in $Cu(In,Ga)Se_2$ based solar cells caused by the (V-Se-V-Cu) vacancy complex, J. Appl. Phys. **100** (2006) 113725.

[22] J. Lauwaert, S. Khelifi, K. Decock, M. Burgelman and H. Vrielinck, Signature of a back contact barrier in DLTS spectra, J. Appl. Phys. **109** (2011) 063721.

[23] J. Lauwaert, L. Callens, S. Khelifi, K. Decock, M. Burgelman, A. Chirila, F. Pianezzi, S. Buecheler, A. N. Tiwari and H. Vrielinck, About RC-like contacts in deep level transient spectroscopy and $Cu(In, Ga)Se_2$ solar cells, Prog. Photovoltaics, **20(5)** (2012) 588594.

[24] K. Decock, J. Lauwaert, and M. Burgelman, Characterization of graded CIGS solar cells, Energy Procedia, **2(1)** (2010) 49-54.

[25] K. Decock, S. Khelifi, M. Burgelman, Analytical versus numerical analysis of back grading in CIGS solar cells, Solar Energy Mater. Sol. Cell., **95** (2011) 1550-1554.

[26] A. Chirilă, D. Guettler, D. Bremaud, S. Buecheler, R. Verma, S. Seyrling, S. Nishiwaki, S. Haenni, G. Bilger, and A. N. Tiwari, Cigs solar cells grown by a three-stage process with different evaporation rates, Proc. 34th IEEE Photovoltaic Specialists Conference, Philadelphia, USA, June 712, 2009, 812-816.

[27] J. Lauwaert, K. Decock, S. Khelifi and M. Burgelman, A simple correction method for series resistance and inductance on solar cell admittance spectroscopy, Solar Energy Mater. Sol. Cell. **94** (2010) 966.

[28] S. Weiss and R. Kassing, Deep level transient fourier spectroscopy (DLTFS)- a technique for the analysis of deep level properties, Solid St. Electron. **31** (1988) 1733.